Title
Differences between FLIM phasor analyses for data collected with the Becker and Hickl SPC830 card and with the FLIMbox card

Journal
Microscopy Research and Technique, 81(9)

ISSN
1059-910X

Authors
Ranjit, Suman
Malacrida, Leonel
Gratton, Enrico

Publication Date
2018-09-01

DOI
10.1002/jemt.23061

Peer reviewed

HHS Public Access

Author manuscript

Microsc Res Tech. Author manuscript; available in PMC 2019 October 08.

Published in final edited form as:

Microsc Res Tech. 2018 September ; 81(9): 980–989. doi:10.1002/jemt.23061.

Differences between FLIM phasor analyses for data collected with the Becker and Hickl 830 BH card and with the FLIMbox card

Suman Ranjit[1,‡], **Leonel Malacrida**[1,2,‡], and **Enrico Gratton**[1]

[1]Laboratory for Fluorescence Dynamics, University of California, Irvine

[2]Departamento de Fisiopatología, Hospital de Clínicas, Universidad de la República, Montevideo, Uruguay

Abstract

The phasor approach to FLIM (Fluorescence Lifetime Imaging Microscopy) is becoming popular due to the powerful fit free analysis and the visualization of the decay at each point in images of cells and tissues. However, although several implementation of the method are offered by manufactures of FLIM accessories for microscopes, the details of the conversion of the decay to phasors at each point in an image requires some consideration. Here we show that if the decay is not properly acquired, the apparently simple phasor transformation can provide incorrect phasor plots and the results may be misinterpreted. In particular, we show the disagreement in experimental data acquired on the same samples using the two cards (FLIMbox, frequency domain and Becker & Hickl BH 830, time domain) and the effect produced by using the BH 830 card with different settings. This difference in data acquisition translates to the assignment of phasor components calculated using different acquisition parameters. This effect is already present in the original data that are not acquired with the proper parameters for the phasor conversion. We also show that the difference in the resolution of components already exists in the data acquired in the time domain when used with settings that do not allow acquisition of the fluorescence decay on a sufficient large time scale.

Graphical abstract

Correspondence to: Enrico Gratton.

‡Contributed equally to this work

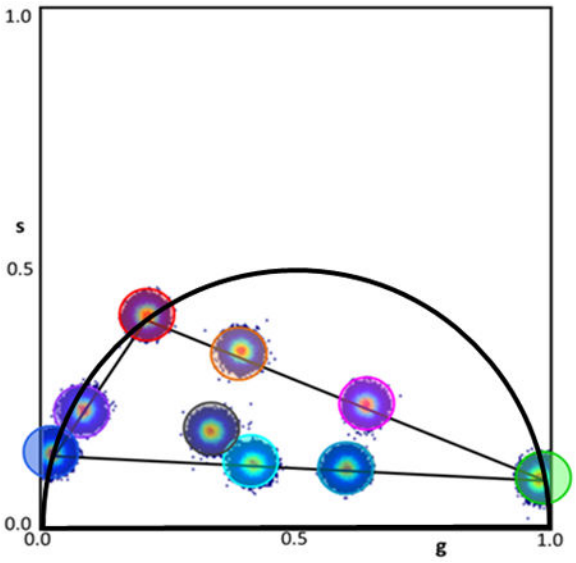

Introduction

The phasor approach to FLIM has become a popular technique in image analysis (Celli and others; Colyer and others, 2009; Fereidouni and others, 2014; Jameson and others, 1984; Malacrida and others, 2016; Sameni and others, 2018; Sena and others, 2017). The phasor approach was originally conceived for analysis of FLIM data in the frequency domain. The equations for conversion of the intensity decay into phasor plots have appeared in several publications (Digman and others, 2008; James and others, 2011; Malacrida and others, 2016; Malacrida and others, 2015; Malacrida and others, 2017; Stefl and others, 2011). Although these equations are deceptively simple, the conditions appropriate for the conversion of data obtained in the time domain (typically Time Correlated Single Photon Counting or TCSPC) to phasors should be carefully considered. This discussion is lacking in the current literature and this paper addresses one specific aspect of the conversion of TCSPC data to phasors which could result in substantial errors in phasor analysis and in the interpretation of the results. This issue applies when FLIM data are acquired with high repetition lasers (typically 80 MHz) and when one part of the decay between pulses is missing. Other issues arises when TCSPC data are not analyzed taking into account of the instrument response function (IRF) and when components with long lifetimes, that are not present in the short record obtained in FLIM measurements, are looked for in the analysis. There is an ample literature describing the use of methods for data collection and analysis for TCSPC data (Becker and others, 2006; Becker and others, 2016). When acquiring TCSPC data for FLIM, problems arise for three reasons: one is the way the phasor transformation is done for TCSPC data, the second is that TCSPC data collected using a high repetition lasers could not contain information about long lifetime decays and the third is that the very early decay, if not properly deconvoluted, could hide the signal due to very short decay components. Traditionally, TCSPC data was acquired from a low repetition rate laser or with the help of a pulse picker to decrease repetition rate. The delay in TAC (time to amplitude converter) has to be long enough to complete the fluorescence lifetime decay. Advent of high repetition rate

laser and measurement in biological sample has started this trend where the TCSPC acquisition is rather short as long acquisitions are detrimental to the sample. Shortening the TAC timescale have resulted in acquisition of incomplete decays and improper conversion to phasor plot.

One important condition for the conversion of decay data from the time domain to phasors is that one entire period of the intensity decay should be available in the time record. If this is not the case, then phasors originating from a single exponential decay could fall inside or outside the “universal semicircle”, giving erroneous results [1]. The law of linear combination of phasors could still be valid but the landmark in the phasor plot, which is the ‘universal semicircle” loses its meaning. The existence of the universal semicircle is dependent on the exponential decay and it only applies to lifetime phasors. For example, there is no universal semicircle for spectral phasors (Digman and others, 2008). A common error in the phasor plots, produced when the original time domain data are not acquired for an entire period, is to assume that a point not on the universal circle arises from a linear combination of multiple decays. Another common experimental error is the lack of relatively short and long lifetime components that are more significant in the early decay and in the late decay in the acquired TCSPC time delay histogram. In this paper we show that those errors can in part be avoided by properly setting the parameter of the BH 830 TCSPC acquisition card (http://www.becker-hickl.com/spc830.htm).

Experimental

Fluorescence lifetime imaging

Samples were measured using a modified Zeiss Axiovert S100TV (Zeiss, Thornwood, NY) microscope equipped with a Spectra-Physics MaiTai HP laser (Spectra-Physics, Santa Clara, CA) for excitation and a photomultiplier tube (H7422P-40, Hamamatsu, Bridgewater, NJ) for detector. The samples were excited with the 780 nm laser line using a 40X water immersion objective (1.2 NA, Zeiss, Thornwood, NY) by two photon excitation. The fluorescence was passed through a filter (350 nm – 700 nm, BG39, Edmund Optics, Barrington, NJ) and collected using the photomultiplier tube (H7422P-40, Hamamatsu, Bridgewater, NJ), and recorded using two different time-resolved methods, FLIMbox (Model A320 ISS, Champaign, IL) and SPC-830 (Becker & Hickl GmbH, Berlin, Germany). The pixel dwell time for the acquisitions was 32 μs and the images were taken with sizes of 256×256 pixels. To have a high signal to noise ratio, 30 – 50 frames were collected. To make comparison between FLIMbox and SPC-830 cards, same number of maximum counts was recorded using each acquisition mode. The data from the each pixel were recorded and analyzed using the SimFCS software (Laboratory for Fluorescence Dynamics, University of California, Irvine, CA). The data collected using the FLIMbox is directly transformed to a phasor plot following the frequency domain approach. Data acquisition using SPC830 or BH card provides the histogram of the TCSPC approach and here the data for TCSPC acquisition followed by phasor transformation was collected using two different set of parameters. In the first set, the gain of the SPC830 was set at 4 given an ADC range of 50 ns (Figure a). This range equates to an acquisition window of 12.5 ns. A part of this time window was not used and the data acquisition was only recorded for an

interval of this time range (red and blue cursors, Figure 1A). This step causes the actual window of acquisition to be ~9 ns which includes the rise time (Figure 1A). The shape of the decay inside this window not cover a period of the laser repetition and the decay is not complete, especially for long lifetimes, and thus transformation to the phasor plot should be done taking into account this effective reduced time window (Fereidouni and others, 2014; Fereidouni and others, 2011). The second acquisition setting for BH card used a gain of 2 and range of 25 ns, resulting in total window of acquisition of 25 ns (Figure 1B). A 12.5 ns window from this 25 ns acquisition window was extracted representing an entire period of the laser repetition and used for the phasor transformation (in between the blue and red cursor, Figure 1B). Figure 1B shows this acquisition scheme and one notes that the 12.5 ns window selected results in a periodic signal and thus proper phasor transformation. The images in this scheme take longer to acquire as the total window of acquisition in this setting is 25 ns. The transformation of the TCSPC data to the phasor plot is explained below.

Conversion to Phasors

The intensity decays $I(t)$ collected at each pixel of the image using the TCSPC approach were transformed to the Fourier space and the phasor coordinates were calculated using the following relations:

$$g_{i,j}(\omega) = \int_0^T I(t) \cdot \ Cos\ (n\omega t)dt / \int_0^T I(t)dt \quad \text{(Eq 1)}$$

$$s_{i,j}(\omega) = \int_0^T I(t) \cdot \ Sin\ (n\omega t)dt / \int_0^T I(t)dt \quad \text{(Eq 2)}$$

where, $g_{i,j}(\omega)$ and $s_{i,j}(\omega)$ are the X and Y coordinates of the phasor plot, respectively, and n and ω are the harmonic number and the angular frequency of excitation, respectively. The transformed data was then plotted in the phasor plot in a way that the data from each individual pixel is transformed to a point in the phasor plot. In this work we use the first and the second harmonics for data analysis.

In frequency domain measurements, the transformation to the phasor plot uses the following relation,

$$g_{i,j} = m_{i,j} .\ Cos\ (\phi_{i,j}) \quad \text{(Eq 3)}$$

$$s_{i,j} = m_{i,j} .\ sin\ (\phi_{i,j}) \quad \text{(Eq 4)}$$

where, $g_{i,j}(\omega)$ and $s_{i,j}(\omega)$ are again the X and Y coordinates of the phasor plot, respectively, and $m_{i,j}$ and $\phi_{I,j}$ are the modulation and phase at the pixel i, j. The distribution of phasor points originating from FLIM measurements appear on (for the mono-exponential decays) or inside (for multiexponential decays) the universal semicircle. The larger phase angle in the phasor plot is indicative of the longer lifetime.

In the phasor approach, the law of linear addition dictates that if the fluorescence decay from a pixel has contribution of two different individual decays then the phasor position originated from this point lies in the line joining the phasor positions of the two independent decays. The distance from the original phasor position of the components to the new position from that pixel is inversely proportional to the fractional intensity contribution of that component. This fact can be shown from the following mathematical deduction:

For a two component system having contribution from two separate mono-exponential decays,

$$I(t) = A_1 e^{-t/\tau_1} + A_2 e^{-t/\tau_2}, \quad \text{(Eq 6)}$$

The calculated phasor positions from this decay assuming that we integrate the time decay from 0 to infinity are,

$$g(\omega) = \left(A_1\tau_1 \frac{1}{1+(\omega\tau_1)^2} + A_2\tau_2 \frac{1}{1+(\omega\tau_2)^2} \right) / (A_1\tau_1 + A_2\tau_2) \quad \text{(Eq 7)}$$

$$s(\omega) = \left(A_1\tau_1 \frac{\omega\tau_1}{1+(\omega\tau_1)^2} + A_2\tau_2 \frac{\omega\tau_2}{1+(\omega\tau_2)^2} \right) / (A_1\tau_1 + A_2\tau_2) \quad \text{(Eq 8)}$$

These equations can be simplified using the definition of the fractional intensity of each of the original components where fractional intensity is $f_i = A_i\tau_i / \Sigma_i A_i\tau_i$

Using this transformation, the phasor coordinates resolve to,

$$g(\omega) = f_1 \frac{1}{1+(\omega\tau_1)^2} + f_2 \frac{1}{1+(\omega\tau_2)^2} \quad \text{(Eq \_9}$$

$$s(\omega) = f_1 \frac{\omega\tau_1}{1 + (\omega\tau_1)^2} + f_2 \frac{\omega\tau_2}{1 + (\omega\tau_2)^2} \quad \text{(Eq 10)}$$

Thus, for phasor coordinates, the exponential components are additive when combined with their relative fractional intensity contribution. This trait is known as the “law of addition of phasors” and is true for multiple decays.

Finally, for multiple decays, phasor coordinate are given by:

$$g(\omega) = \sum_j f_j g_j(\omega) \quad \text{(Eq 11)}$$

$$s(\omega) = \sum_j f_j s_j(\omega) \quad \text{(Eq 12)}$$

This results in ‘law of phasor addition’, in which the relative contribution of two or more phasor points towards another point in between them are inversely proportional to the distances between the point in the middle and their corresponding phasor points. A three component system results in the new phasor position to be inside the triangle formed by phasor positions of the corresponding individual decays.

Materials and methods

9, 10(H) Acridanone, Rhodamine 110 and Coumarin 6 were purchased from Sigma-Aldrich (St. Louis, MO) and Cy3 was purchased from Lumiprobe (Hunt Valley, MD). Acridanone, Rhodamine 110 and Cy3 solutions were prepared by dissolving the solid in PBS buffer (pH=7.4) (Sigma Aldrich, St. Louis, MO) and diluting them to the proper concentration (~ 10 to 20 μM). Coumarin 6 was dissolved in ethanol (Sigma-Aldrich, St. Louis, MO) and diluted to the final concentration of 20 μM. The solutions in PBS are then mixed together to create mixtures used for the experiments. The following sets of solutions were created: two sets of Cy3 and Rhodamine 110 mixture; two sets of Cy3 and 9, 10(H) Acridanone mixture; one set of Rhodamine 110 and 9, 10(H) Acridanone mixture, and a three component mixture consisting of Rhodamine 110, Cy3 and 9, 10(H) Acridanone in the same proportion as that of one set of two-component mixtures. Coumarin 6 in ethanol was used for calibration of the phasor plot as it has a mono-exponential lifetime of 2.5 ns. *Convallaria majalis* (MEDICAL & SCIENCE MEDIA, N.S.W, Australia) rhizome with concentric vascular bundles sample was used for autofluorescence imaging with 780 nm excitation to separate out different lifetime contributions and calculate and compare the phasor position obtained from various different types of acquisitions. The samples were placed 35-mm MatTek glass-bottom dishes (MatTek Corporation, MA) and dish was placed on top of the objective.

The fitting of the TCSPC data is done by moving the maxima of the exponential decay to time = 0, and then fitting with mono-exponential or bi-exponential decays. Origin 9.0 (OriginLab, Northampton, MA) was used for the plots of the fluorescence lifetime decays and fitting and minimization of the residuals were obtained using Levenberg–Marquardt algorithm. The decays were fitted without deconvolution from the instrument response function (IRF)

Results

Systems composed of 3 single exponential decay components and their mixture acquired with the FLIMbox card

The original “images” of the solutions are shown in Figure 2 for the nine samples. The instrument was calibrated using a solution of Coumarin 6 as described in the Methods section. All phasor clusters are on the universal semicircle for the pure single exponential components and inside the universal semicircle for the mixtures. The colors of the images correspond to the color of the cursor used in the phasor plot shown in Figure 2. Note that all the phasor clusters have about the same circular shape since all data where acquired with equal number of photons.

The mixtures of components are aligned along the line of linear combination joining the phasor of the pure components. If the mixture contains mixtures of components as shown in figure 2-I, the phasors of these mixtures are in the line joining the phasors of the components. The graphical solutions for the fraction of the components for the mixtures in Figure 2 are given in the caption of figure 2.

The effect of the number of counts on the phasor distribution is shown in Figure 3.

The same solutions were measured with the BH 830 card using a gain of 4 and a gain of 2 and using the region of the decay discussed in Figure 1. The color of the phasor clusters is the same used for Figure 2.

As shown in Figure 4, the position of the phasors clusters in the phasor plot depends on the calibration and on the acquisition of the entire period rather than just a portion of the period as discussed in Figure 1. The calibration was done using Coumarin 6 which has a single exponential lifetime of 2.5 ns. The phasors that are in the proximity of the phasor used for the calibration are less affected than the phasors which are very different such as these for Cy3. Figure 4A shows that the position of the phasors can be outside the universal circle if the BH SPC830 card is set to a gain of 4 for the laser repetition period of 12.5 ns. This setting prevents the acquisition of the entire period between 2 pulses as shown in Figure 1A.

For a sample which displays many components such as the Convallaria slide frequently used for calibration in microscopy, the entire phasor distribution is found at a different location using a gain of 4 compared to the phasor plot obtained with a gain of 2.

As shown in figure 5C the phasor distribution is shifted to shorter phase with respect to the same data taken with a gain of 4, which could result in serious misinterpretation of the results.

The purpose of this paper is to show that the advantages of the phasor fit free approach can vanish if the phasor transformation is not done with data acquired in entire period of the laser repetition rate. In Figure 4A we show that the phasor transformation done using the BH SPC830 card with a gain of 4 can give points that are outside the universal semicircle which should never happen for samples with non-interacting species (or species experiencing excited state reactions). Clearly, if the points are in the wrong location in the phasor plot, the methods for the analysis of the phasor plot for FRET, multispecies analysis and metabolic trajectories will produce erroneous results.

In this paragraph we analyze another issue which is independent of the data transformation to phasors and it has to do with the contribution of long and short lifetime components when the entire decay is not measured and the initial part of the decay curve is not analyzed since it will require deconvolution of IRF from the decay curve, which is usually not done for FLIM images. This discussion applies to data obtained for FLIM with high repetition lasers, although it has an affect also if the laser repetition rate is 40MHz and lifetimes are in the 8-10 ns range. Here we also compare the capability of the phasor analysis to recover lifetime components with respect to fitting algorithms. For the analysis of the decay curve in the time domain, we consider the results of algorithms based on ignoring the early part and the decay at longer times on the resolution of components, commonly used for FLIM data. We also average the decay at each point of an image (for the solution samples) so that the S/N ratio allows performing a simple fit of the decay curve.

The graphical method to determine the lifetime of components using the phasor plot

The phasor approach offers a fit free method to determine the lifetime value of components based on their position in the phasor plot. If the decay is single exponential, the corresponding phasor should be located on the universal semicircle. Then by determining the phase and modulation of the position of the phasor in the phasor plot, the single exponential value can be obtained with a simple calculation based on the value of the phase or modulation. Since the error on the value depends only on the square root of the number of photon collected, the value as well as the error can be evaluated directly from the phasor plot. The center of the distribution has a very small error since it is the result of many independent determinations (for the solutions and mixture samples) and this error can directly propagate to the lifetime values (Gratton and others, 1984).

In the case of a mixture of two components, we use a graphical method to extract the value and fractional intensities of the two components using the position of the phasor in the first and second harmonic phasor plot. The graphical algorithm is shown in Figure 6. The algorithm searches the points T1 and T2 on the universal semicircle that give a line that simultaneously passes through the experimental point P in the phasor plots of the first and second harmonics. In the phasor plot of the first and second harmonic, we mark the position of the center of the phasor distribution of the mixture. Then a search is done for two lifetime components that are compatible with these two phasors positions. This search is very fast and as a result we obtain the two lifetime values and fractional intensities of the mixture. Another alternative could be to resolve the non-linear equations given by the coordinates of

the phasor component, but this approach is a return to the fitting procedures which is avoided in the phasor approach.

The error in the resolution of the component's lifetimes and fractional intensities can be obtained by exploring the region around the points P that contain 68% of the experimental points and determining the maximum and minimum values of T1, T2 and F1 (the fractional intensity of component 1) compatible with this search. These errors ultimately depend on the width of the phasor clusters around P. As previously discussed, this width is a function of the number of photon collected, but the width is independent on the location of the phasor in the phasor plot.

The phasor representation of the decay offers a simple algorithm to decrease the width of the phasor cluster as shown in figure 7. The algorithm is based on the application of the median filter to the images of the G and S coordinates. This algorithm is not affecting the image resolution, but only the coordinates used in the phasor plot.

Resolution of components

Failure to detect very short and long lifetime components: analysis using the fit of a part of the decay curve for gain of 4 and gain of 2 for the BH 830 card and comparison of the resolution of two components using the phasor method.

Additional insight about the deformation of the data cause by the lack of using the initial and final part of the decay curve can be gained by using fitting algorithms to extract exponential components from the data, which are usually used for FLIM data analysis. We want here to reiterate that there is nothing wrong with the collection of data using the TCSPC method and the methods for the analysis of TCSPC data. Our concern is that the “usual” analysis performed on FLIM data acquired using a high repetition rate laser is affected by large systematic errors that can lead to erroneous interpretation of the data. However, if the original TCSPC data are collected with wrong setting for the conversion to phasors, the conversion to phasors will not “fix” the original error. The data will be erroneously placed in the phasor plot and the interpretation of the decay in terms of molecular species can be wrong. In part, these systematic effects can be diminished in the phasor approach if data collection is done “properly”, which means collecting at least one entire period of the intensity decay at each pixel. Our second point is that the phasor approach, which is not attempting to resolve the decay into exponential, is not affected by the same error than the traditional analysis of exponential components which appears when FLIM data are collected in a FLIM system using high repetition rate lasers.

Table 1 shows the analysis of single decay components using the graphical phasor method. In this case we obtain the “expected” values of the components using data from a BH 830 card with a gain of 4, a gain of 2 and using the data from the FLIMbox and the phasor method. In the case of Cy3 collected with a gain of 4 in the BH 830 card, the phasor analysis cannot be performed. Since the phasor method is a graphical determination of the positon of the phasor on the universal semicircle, it gives values in agreement for medium and long

lifetime species, but it cannot resolve a species that is outside the universal semicircle such as for Cy3 with data collected with a gain of 4.

For the single component samples, Table 2 shows that the analysis using fits differ somehow from the phasor analysis. For the data acquired with a gain of 4 for the BH830 card, the results differ from the expected values much more than for the data acquired with a gain of 2 with the same card. We believe that this difference is due to the lack of the IRF deconvolution and the wrong estimation of the long lifetime components, since the record of the decay is quite incomplete for this case.

For the mixtures, the recovered values for the components using the fits are all over the map. As reported in Table 3, the long component of 9-10 H Acridanone is recovered poorly using the fit method as well as that of the other components. The analysis of data using a gain of 2 are more in line with the expected values only if the lifetime values are fixed during the fit. Given the statistics used for data acquisition in this work (maximum 500 counts/pixel), it appears that the analysis of a mixture of two components in FLIM cannot be done unless the values of the components are fixed, which means that they must be known separately.

Table 4 shows that the graphical phasor approach applied on the same data set used for table 3 is more consistent in recovering the lifetime of the components of the mixtures and the values for the exponential components recovered are similar to the values obtained using the FLIMbox method of data collection.

Discussion and Conclusion

Data collected using TCSPC or other time domain methods when transformed into phasors could lead to distorted phasor plots as shown in this study. In our example case, data are collected with a gain of 2 and a gain of 4 in the BH 830 card. Using a gain of 2, less distorted plots can be obtained. We explain the reason for this effect is the lack of data acquisition in a sufficient range to cover at least a period of the intensity decay. Note that a gain of 4 is what is recommended by for this card using high repetition lasers. Therefore, the use of phasor analysis with this card requires changing the default setting, which is rarely done.

A different but important issue arising with FLIM data acquired for only a portion of the laser period and analyzed using only a selected part of the decay is the distortion and suppression of very short and very long components. The very short lifetime components presumably can be recovered using deconvolution of the IRF in the time domain, but the long components are lost if only a part of the decay is recorded. We analyzed the effect of the reduced recording range and we found that the missing components cannot be recovered reliably when data were collected with a gain of 4. However, using a gain of 2 in the BH 830 card, transforming the data to the phasor plot and analyzing the data using the first and second harmonic of the phasor conversion of the TCSPC data, the lifetime and amplitude of species in a mixture of 2 components are reliably recovered as shown in the Table 4. We note that the recovery of the lifetime of Cy3 in the mixtures is always on the longer lifetime side, presumably because the IRF was not deconvoluted. Instead the long lifetime

component of 9, 10 H Acridanone cannot be recovered in the mixture with Rhodamine 110. This failure is due again to the reduced time range of data acquisition that limits the long recover of long lifetime components. However, in the phasor plots of figure 2 and 4, the phasor of the mixtures clearly moves towards the 9, 10 H Acridanone when this species is present. This observation points out that the existence of long lifetime components can be seen in the phasor plots but not in the components recovered by data fitting

Although for the example for this paper we used the Becker and Hickl 830 card, a similar effect as discussed in this work will affect data acquired with other cards unless the cards are set to acquire an entire period of the laser repetition or if lower repetition frequency lasers are used. For FILM analysis of autofluorescence of cell and tissue, high rep rate Titanium-Sapphire lasers are used which will give rise to the effect discussed in this paper. The use of phasor analysis will not fix the original problem unless the cards employed are capable of measuring the decay of the entire laser period. If the original data are acquire properly using the decay over a laser period, the fit free approach and the intrinsic correction for the IRF offered by the phasor analysis could make the analysis of FLIM data easy to use and more importantly, free of artifacts.

Acknowledgments

This work was supported in part by grants NIH P41-GM103540 and NIH P50-GM076516. LM is in part supported by the Universidad de la Republica-Uruguay as a full time professor.

References

Becker W, Bergmann A, Haustein E, Petrasek Z, Schwille P, Biskup C, Kelbauskas L, Benndorf K, Klocker N, Anhut T, Riemann I, Konig K. Fluorescence lifetime images and correlation spectra obtained by multidimensional time-correlated single photon counting. Microsc Res Tech. 2006; 69(3):186–95. [PubMed: 16538624]

Becker W, Hirvonen LM, Milnes J, Conneely T, Jagutzki O, Netz H, Smietana S, Suhling K. A wide-field TCSPC FLIM system based on an MCP PMT with a delay-line anode. Rev Sci Instrum. 2016; 87(9):093710. [PubMed: 27782585]

Celli A, Sanchez S, Behne M, Hazlett T, Gratton E, Mauro T. The epidermal Ca(2+) gradient: Measurement using the phasor representation of fluorescent lifetime imaging. Biophys J. 98(5): 911–21.

Colyer R, Siegmund O, Tremsin A, Vallerga J, Weiss S, Michalet X. Phasor-based single-molecule fluorescence lifetime imaging using a wide-field photon-counting detector. Proc Soc Photo Opt Instrum Eng. 2009; 7185(71850T)

Digman MA, Caiolfa VR, Zamai M, Gratton E. The phasor approach to fluorescence lifetime imaging analysis. Biophys J. 2008; 94(2):L14–6. [PubMed: 17981902]

Fereidouni F, Blab GA, Gerritsen HC. Phasor based analysis of FRET images recorded using spectrally resolved lifetime imaging. Methods and Applications in Fluorescence. 2014; 2(3)

Fereidouni F, Esposito A, Blab GA, Gerritsen HC. A modified phasor approach for analyzing time-gated fluorescence lifetime images. J Microsc. 2011; 244(3):248–58. [PubMed: 21933184]

Gratton E, Jameson DM, Hall RD. Multifrequency phase and modulation fluorometry. Annu Rev Biophys Bioeng. 1984; 13:105–24. [PubMed: 6378065]

James NG, Ross JA, Stefl M, Jameson DM. Applications of phasor plots to in vitro protein studies. Anal Biochem. 2011; 410(1):70–6. [PubMed: 21078289]

Jameson DM, Gratton E, Hall R. The measurement and analysis of heterogeneous emissions by multifrequency phase and modulation fluorometry. App Spec Rev. 1984; 20:55–106.

Malacrida L, Astrada S, Briva A, Bollati-Fogolin M, Gratton E, Bagatolli LA. Spectral phasor analysis of LAURDAN fluorescence in live A549 lung cells to study the hydration and time evolution of intracellular lamellar body-like structures. Biochim Biophys Acta. 2016; 1858(11):2625–2635. [PubMed: 27480804]

Malacrida L, Gratton E, Jameson DM. Model-free methods to study membrane environmental probes: a comparison of the spectral phasor and generalized polarization approaches. Methods Appl Fluoresc. 2015; 3(4):047001.

Malacrida L, Jameson DM, Gratton E. A multidimensional phasor approach reveals LAURDAN photophysics in NIH-3T3 cell membranes. Sci Rep. 2017; 7(1):9215. [PubMed: 28835608]

Sameni S, Malacrida L, Tan Z, Digman MA. Alteration in Fluidity of Cell Plasma Membrane in Huntington Disease Revealed by Spectral Phasor Analysis. Sci Rep. 2018; 8(1):734. [PubMed: 29335600]

Sena F, Sotelo-Silveira M, Astrada S, Botella MA, Malacrida L, Borsani O. Spectral phasor analysis reveals altered membrane order and function of root hair cells in Arabidopsis dry2/sqe1-5 drought hypersensitive mutant. Plant Physiol Biochem. 2017; 119:224–231. [PubMed: 28910707]

Stefl M, James NG, Ross JA, Jameson DM. Applications of phasors to in vitro time-resolved fluorescence measurements. Anal Biochem. 2011; 410(1):62–9. [PubMed: 21078290]

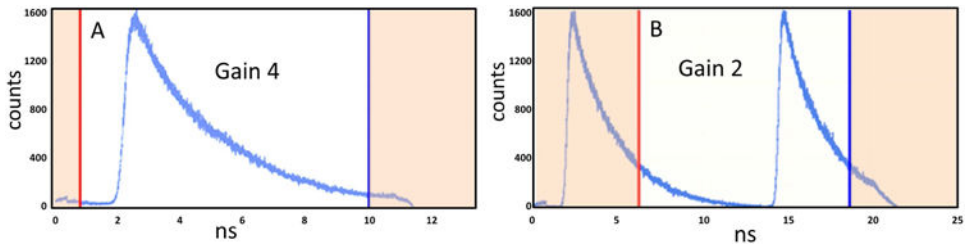

Figure 1.

BH 830 card acquisition of the decay of a solution of Rhodamine 110 excited with a high rep laser at 80 MHz with two different settings of the card. (A) Gain of 4 gives a TAC time range of 12.5 ns. Due to the non-linearity of the TAC at early and later times, only one portion of the decay, indicated by the red and blue lines, is valid giving a total range of about 9 ns, which is insufficient to cover an entire period of the laser. (B) Setting the gain at 2 gives a total larger range (25 ns) but only one part corresponding to 12.5 ns is used (indicated by the red and blue lines) which covers an entire period of the excitation laser. The grayed parts of the decay are not used.

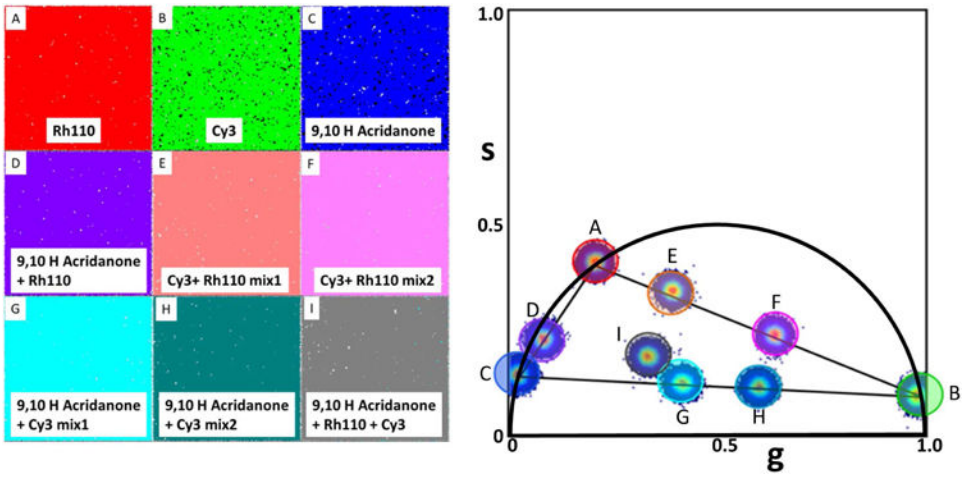

Figure 2.

Data acquired with the FLIMbox card in the frequency domain, directly as phasors. Data were obtained for A) solution of Rhodamine 110 (red circle). B) Cy3 (green circle) and C) 9-10 H Acridanone (blue circle) and their mixtures. D) Mixture of Rho110 and 9-10 H Acridanone. E) Rho 110 and Cy3 Mix 1. F) Rho 110 and Cy3 Mix 2. G) 9-10 H Acridanone and Cy3 (mix1). H) 9-10 H Acridanone and Cy3 (mix2). I) Mixture of 9-10 H Acridanone, Rho 110 and Cy3. The graphical solution for the fraction of the components for the mixtures in Figure 2 are: (D) F(9-10 H Acridanone)=0.705, (E) F(Cy3)=0.228, (F) F(Cy3)=0.556, (G) F(Cy3)=0.405, (H) F(Cy3)=0.598, (I)-F9Rhodamine)=0.177, F(9-10 H Acridanone)=0.519, F(Cy3)=0.304.

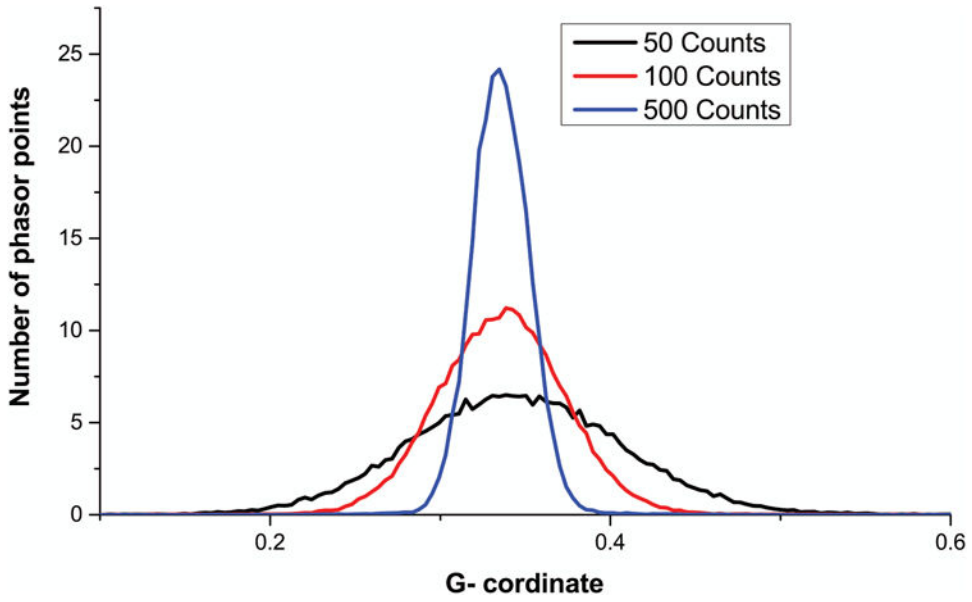

Figure 3.

Effect of the number of photons/pixel on the width of the phasor distribution for data acquired with the FLIMbox. Only the coordinate G is shown since the phasor distribution are symmetrical. Note that width of the phasor distribution is independent on the position of the phasor in the phasor plot but only depends on the number of photon acquired for a given pixel. For this figure we use the mixture of 3 components to show that the composition of the phasor does not affect the cluster distribution.

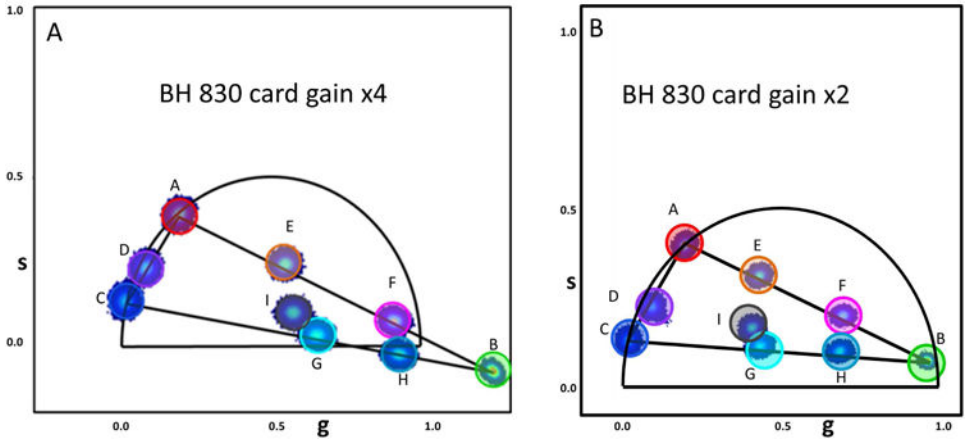

Figure 4.

Effect of gain of the BH 830 card on the location of the phasors of single exponential decay and of mixtures. The Calibration of the phasor plot is done using the Coumarin 6 standard with lifetime of 2.5ns. The labels of the phasor clusters is the same used in Figure 2. A) Solution of Rhodamine 110. B) Cy3. C) 9-10 (H) Acridanone. D) Mixture of Rho110 and 9-10 (H) Acridanone. E) Rho 110 and Cy3 Mix 1. F) Rho 110 and Cy3 Mix 2. G) 9-10 H Acridanone and Cy3 (mix1). H) 9-10 (H) Acridanone and Cy3 (mix2). I) Mixture of 9-10 (H) Acridanone, Rho 110 and Cy3.

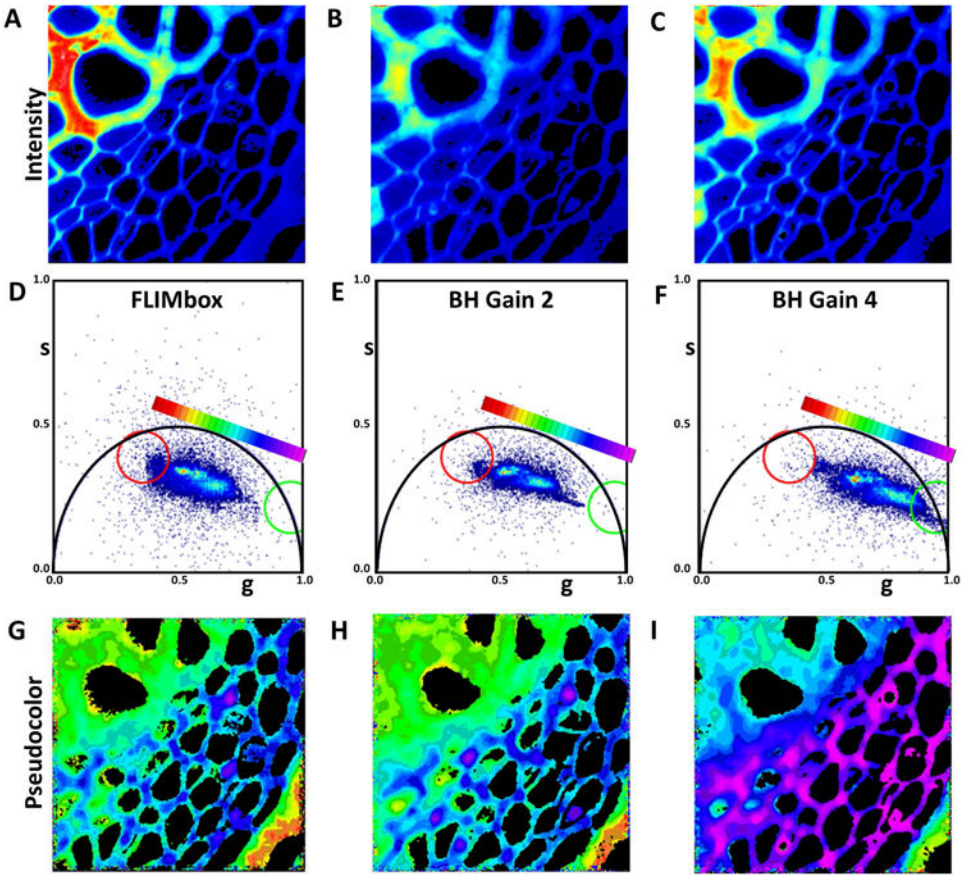

Figure 5.

Convallaria sample and phasor distribution. (A) Image obtained with FLIMbox and (B) using BH SPC830 card with a gain of 4 and (C) using a gain of 2. (D)Phasor distribution for the corresponding instrument settings. G-I) Corresponding color mapped FLIM images. The color map for the phasor distribution is shown in (D-F). The results show that FLIM acquisition with FLIMbox and BH SPC830 card with a gain of 2 give similar phasor plot. The phasor distribution and hence, the color map is completely different for gain of 4.

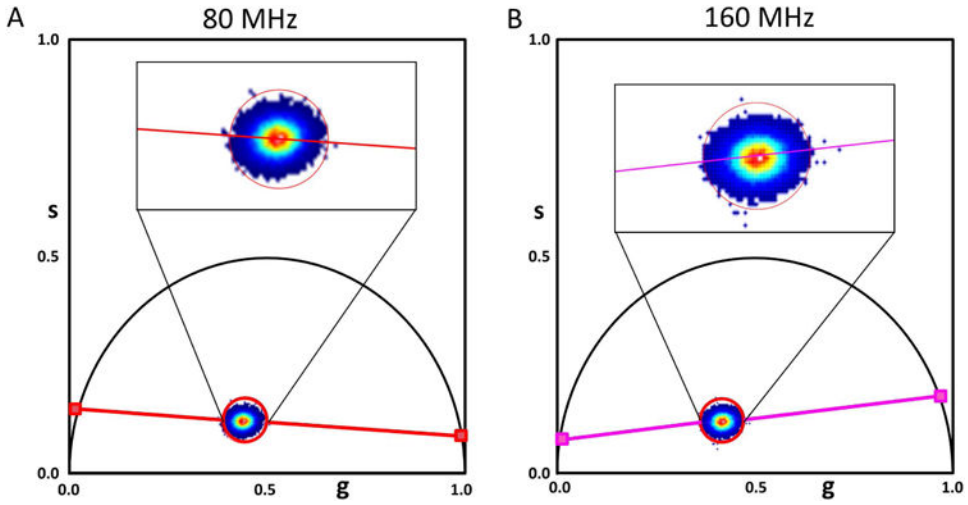

Figure 6.

Graphical solution of two-exponential components mixture using the phasor plot of the first (A) and (B) second harmonics at 80 MHz and 160 MHz, respectively. An experimental phasor point P is shown in the first and second harmonic plots. The graphical algorithm searches for the pair of lifetimes T1 and T2 that determine the line that simultaneously passes through P in both plots. The inset in (A) and (B) is the zoom of the data points in P and the line (red line) passing through the center of P for the first and second harmonics, respectively.

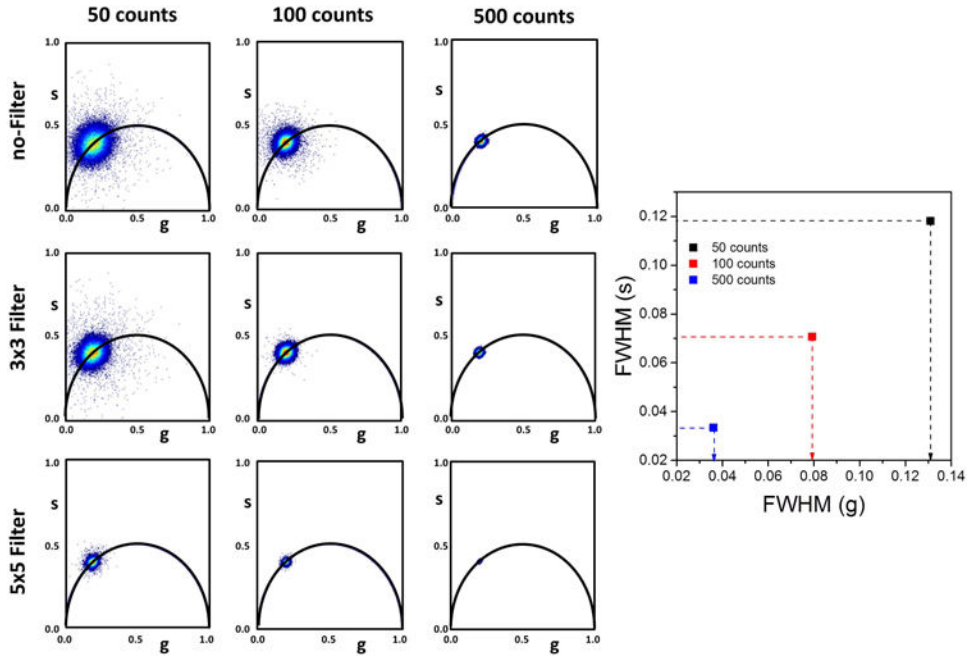

Figure 7.

Effect of the number of counts on the width of the phasors cluster and the action of the median filter in reducing the spread of the cluster. Data is shown here for Rhodamine 110, single exponential collected with the BH SPC830 card, gain 2. The expected value for this dye measured at 80 MHz is Phase= 63.9 Mod= 0.448 TP= 4.056 ns TM= 3.969 ns. These values are obtained at the 3 counting rates, whether the median filter is applied or not. Panels (A), (B) and (C) show the effect of the number of photons collected per pixel on the phasor cluster. Data are summarized in graph (J), where FWHM (full width at half maxima) of the distribution in S and G co-ordinates are plotted. The results of the application of a median filter 3×3 and 5×5 are shown in panels (D), (E), (F) and (G), (H) and (I), respectively.

Table 1

Lifetimes of solutions with a single exponential component acquired with different methods analyzed by the graphical phasor method.

Lifetimes in ns	BH 830 gain of 4	BH 830 gain of 2	FLIMbox
Cy3	Outside the plot	0.19±0.01	0.25±0.01
Rhodamine 110	4.04±0.01	3.98±0.01	4.00±0.02
9, 10(H) Acridanone	14.3±0.1	14.0±0.1	14.0±0.1

Table 2

Solutions of single exponential components analyzed by fitting the decay curve for single exponentials. The first and last part of the curve was not used. No deconvolution for the IRF was applied.

Sample	Gain	τ (ns)	Comments
Rhodamine 110	4	5.708 ± 0.054	Gain 4 has worse result than gain 2
Rhodamine 110	2	4.377 ± 0.021	
Cy3	4	0.325 ± 0.006	Gain 4 has worse result than gain 2
Cy3	2	0.276 ± 0.005	
9, 10 (H) Acridanone	4	33.640 ± 5.975	Gain 4 has worse result than gain 2
9, 10 (H) Acridanone	2	17.717 ± 0.858	

Table 3

Mixtures of two components analyzed using 2 exponential fits without IRF deconvolution.

SaSample	Gain	T1 (ns)	A1	T2(ns)	A2	Comments
Rh110+Cy3 m1	4	0.351 ± 0.006	0.922	8.731 ± 1.532	0.267	Gain 4 results in wrong long lifetime, Gain 2 gives reasonable values for Rhodamine 110 and Cy3
Rh110+Cy3 m1	2	0.279 ± 0.005	0850 ± 0.008	4.596 ± 0.245	0.253 ± 0.003	
Rh110+Cy3 m3	4	0.335 ± 0.005	1.164	35	0.182	With Gain 4, this sample cannot be fitted with unconstrained bi-exponentials. The longer lifetime was fixed. Gain=2 doesn't have this problem
Rh110+Cy3 m3	2	0.270 ± 0.004	1.030 ± 0.008	6.675 ± 1.891	0.072 ± 0.006	
9, 10 (H) Acridanone + Rh110	4	7.421 ± 0.167				For both gains, 2-exponential and 2-exponential samples have similar distribution of residuals. With gain 4, the unconstrained 2-exponential fitting fails. With gain 2, 2-exponential fits can only be obtained with fixed lifetimes.
9, 10 (H) Acridanone + Rh110	2	5.905 ± 0.006				
9, 10 (H) Acridanone + Cy3 m2	4	0.338	1.085	11	0.042	In both gain 4 and gain 2, the longer lifetime needed to be fixed. However, the errors of measurements (not shown) are smaller using gain 2.
9, 10 (H) Acridanone + Cy3 m2	2	0.275	1.0596	11	0.065	
9, 10 (H) Acridanone + Cy3 m3	4	0.351 ± 0.006	1.760	11	0.007	In both gain 4 and gain 2, the longer lifetime need to be fixed. The errors (not shown) are smaller with gain 2.
9, 10 (H) Acridanone + Cy3 m3	2	0.270 ± 0.004	1.088	11	0.020 ± 0.055	

Table 4

Phasor analysis of 2-component mixtures using first and second harmonics of the TCSPC data acquired with a gain of 2 in the BH 830 card. The components fractional intensities are normalized.

Mixture	T1 (ns)	F1	T2 (ns)	F2
Rho 110+cy3 Mixture 1	0.15±0.02	0.288±0.005	3.82±0.43	0.717±0.005
Rho-110+cy3 Mixture 3	0.15±0.02	0.622±0.005	3.71±0.39	0.378±0.005
9,10 H-Acridanone+Cy3 Mixture 2	0.165±0.06	0.431±0.005	13.03±0.16	0.569±0.005
9,10 H-Acridanone+Cy3 Mixture 3	0.165±0.03	0.688±0.005	11.91±0.46	0.312±0.005
9, 10(H) Acridanone+Rh110	4.308±0.05	0.488±0.005	21±1.0	0.512±0.005